2008 IEEE International Conference on
Robotics and Automation
Pasadena, CA, USA, May 19-23, 2008

Modeling of a Closed Loop Cable-Conduit Transmission System

Varun Agrawal, William J. Peine, Bin Yao

Abstract— **Many surgical robots use cable-conduit pairs in a pull-pull configuration to actuate the instruments and transmit power into the patient's body. Friction between the cable and the conduit makes the system nonlinear and accounts for major losses in tension transmission across the cable. This paper proposes an analytical model for a similar cable-conduit system and formulates the load transmission characteristics. The dynamic model uses discrete elements with friction losses and cable stretch calculated for each of the segments. The simulations predict backlash, cable slacking, and other nonlinear behavior. These results are verified with an experiment using two DC motors coupled with a cable-conduit pair. The drive motor is run in position control mode, while the load motor simulates a passive environment torsional spring. Experimental results are compared with the simulation and various implications are discussed.**

I. Introduction

SURGICAL robots often utilize cable-conduit pairs in a pull-pull configuration to actuate the patient-side manipulators and slave instruments [1, 2]. Cable transmissions are preferred because they can provide adequate power through narrow pathways and allow the actuators to be located safely away from the patient. Control of these systems, however, is challenging due to cable compliance and friction within the conduit. These nonlinearities introduce significant tension losses across the cable and give rise to motion backlash, cable slack, and input dependent stability of the servo system [3, 4]. Moreover, frictional forces are directly dependent on the pretension in the cables and the curvature of the conduits.

Previous research in cable-conduit mechanisms has focused on characterization of the friction effects and control of robotic hands. Kaneko et al. [5, 6] analytically calculated the equivalent cable stiffness for a single cable using a force balance on a differential cable element with Coulomb friction. Furthermore, the authors proposed a lumped mass model for tension transmission across the cable. Similar force transmission models have been used by Palli et al. [7, 8] with a continuous Karnopp friction model. These authors also presented control strategies for the system. In both of these cases, the focus of the research has been on a single cable for power transmission. In contrast, Kaneko et al. [3] have performed experiments on torque transmission from the actuator to the finger joint using a pair of cables. These experiments assumed a large value of pretension in the cable to avoid any slacking. In addition, a model for torque transmission for the actuator to the load using a pair of cables has not been developed.

The present work considers the complex interaction between a pair of pull-pull cables in a closed-loop configuration with any level of pretension. An analytical model is developed using discrete cable elements to solve for the nonlinearities present in the system and predict cable slacking and overall transmission characteristics of the system. The model is validated through experiments. In the paper, the setup of the problem is discussed followed by details of the model and the simulation results. The methodology of experiments is outlined and experimental results are presented and compared with the simulation results.

Manuscript received September 14, 2007

V. Agrawal is with Department of Mechanical Engineering, Purdue University, West Lafayette, IN47906 USA (e-mail: vagrawal@purdue.edu).

B. Yao is with School of Mechanical Engineering, Purdue University, West Lafayette, IN 47906 USA (e-mail: byao@purdue.edu).

W. J. Peine is with School of Mechanical Engineering, Purdue University, West Lafayette, IN 47906 USA (phone: 765-494-5626; e-mail: peine@purdue.edu).

II. Motivation and Setup

In surgical robots, the patient side manipulators are mechanically actuated using cable drives passing through a thin tube or conduit [1, 2]. Nonlinearities and backlash are introduced in the motion transmission characteristics due to the friction forces between the cable and the conduit. Moreover, tension losses across the cable necessitate much higher actuating forces for relatively small loads. Since it is difficult to place sensors at the distal ends of the instruments, the position and applied forces of the tool tip are difficult to estimate and control. Hence, the resulting accuracy of the system is extremely poor compared to industrial robots. This results in continuous adjustment of the actuating input by the human in the loop. The objective of this research is to model such a system and characterize the load and motion transmission from the actuator to the load. Ultimately, these models can be used to improve the control strategy of the system.

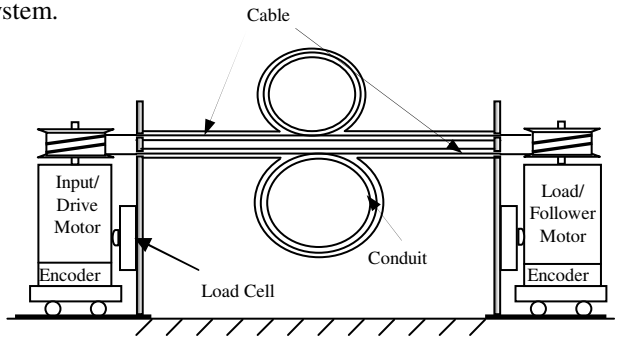

Fig 1: Schematic of the experimental setup

A typical load actuation system of a surgical robot has been emulated in the present experimental setup using a two cable pull-pull transmission actuated with two brushed DC motors mounted on linear slides, as shown in Fig. 1. The first motor is controlled as the input or the drive motor, while the second motor emulates a passive load or environment. Each cable passes through a flexible conduit and is wrapped around pulleys attached to each of the DC motors. The tightly wound spring wire conduits are fixed at each end using two plates attached to the same platforms on which the linear slides are mounted. In this way, the platforms holding the plates are free to move in space, and applying a tension in the cable is counteracted by a compression in the conduit with no forces being transmitted through ground. The cable and the conduit therefore act as springs in parallel.

The actuator or drive motor is run in position control mode while the follower motor is run in torque control mode. The load is simulated as a torsional spring such that the restoring torque applied by the motor is proportional to the angle of rotation. Encoders are used to measure the angular rotation of the two motors. The current flowing across the two motors is measured to estimate the torque applied by the pulley or difference in the two cable tensions. The sum of the two cable tensions is measured using load cells mounted between the linear slide and conduit termination plate. Using the torque values and the load cell measurements, tension at the two ends of each cable can be calculated.

III. Dynamic Model

A. System Governing Equation

Consider an infinitesimal cable segment [*x, x+dx*] with negligible inertia and Coulomb friction acting on it due to contact with the conduit. For this small segment the radius of curvature can be assumed to be constant *R(x),* where *x* is the distance of a point along the conduit. Define *u(x,t)* as the axial displacement of the cable, *T(x,t)* as the axial cable tension in the. N(x,t) denotes the normal force between the cable and the conduit and f(x,t) denotes the frictional force acting on the cable.

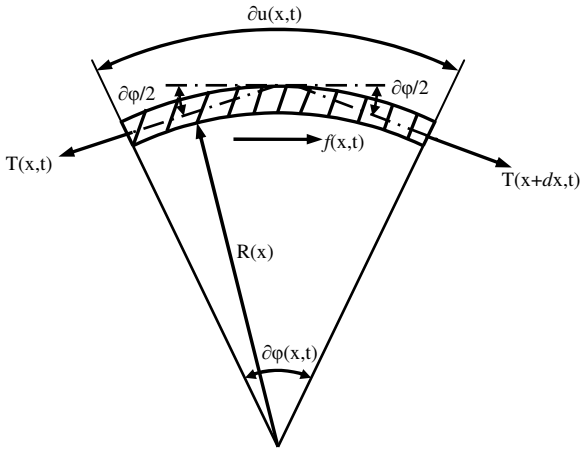

Fig 2: Forces acting on a cable element

When the net axial tension force *T(x+dx,t)-T(x,t) = T'(x,t)dx* is less than the limiting value of friction the cable segment will not move due to the Coulomb friction, i.e.

$$\forall\, x\ s.t.\ \frac{\mu \mathrm{T}}{\mathrm{R}} > \left|\mathrm{T}'(\mathrm{x,t})\right| \Rightarrow \dot{u}(x,t) = 0 \ and\ f(x,t) = \mathrm{T}'(\mathrm{x,t})\mathrm{dx} \quad (1)$$

On the other hand, when the cable segment moves due to the net axial tension, by force balance along the axial direction:

$$T'(x,t)dx = \frac{\mu T}{R} sign(\dot{u})dx \quad when\ \ \dot{u} \neq 0 \quad (2)$$

To calculate the cable strain Hooke's law of elasticity is used, modeling cable-conduit system as a linear spring with stiffness k_{eq}. The governing strain equation is given by:

$$\varepsilon(\mathrm{x,t}) = \frac{T(\mathrm{x,t})}{K} \quad (3)$$

where k_{eq} defines the equivalent stiffness of the cable-conduit system give by:

$$\frac{1}{k_{eq}} = \frac{1}{k_{cable}} + \frac{1}{k_{conduit}} \quad (4)$$

B. Discrete Element Model

Partial differential equations in (1) to (3) define the dynamics of the system. However, due to the discontinuous nature of the friction present in the system, it is difficult to solve the equations. Therefore, for computational simplicity, a discrete element formulation is used by dividing the cable into *n* segments and calculating the displacement and tension of each node at discrete time instants. Consider the i^{th} cable segment between nodes *i* and *i+1*. Let $T(x_i,t_j)$ and $u(x_i,t_j)$ be the tension and the displacement of the i^{th} node, respectively at time t_j. We neglect small variations in radius of curvature over the cable segment, and denote the radius by $R(x_i)$. Based on the motion, cable segments can be divided into three different categories.

Case 1: When the entire cable segment is moving, since $\dot{u}(x,t) \neq 0$, (2) can be integrated to relate the tension and displacements at the two ends as:

$$T\left(x_{i+1},t_j\right) = T\left(x_i,t_j\right)\cdot \exp\left[\frac{\mu\left(x_{i+1}-x_i\right)}{R\left(x_i\right)} sign\left(u(x_i,t_j)-u(x_i,t_{j-1})\right)\right] \quad (5)$$

$$u(x_{i+1},t_j)-u(x_i,t_j) = \frac{R\left(x_i\right)}{k_{eq}\mu} sign\left(u(x_i,t_j)-u(x_i,t_{j-1})\right)\bullet$$
$$T\left(x_i,t_j\right)\exp\left[\frac{\mu\left(x_{i+1}-x_i\right)}{R\left(x_i\right)} sign\left(u(x_i,t_j)-u(x_i,t_{j-1})\right)\right] \quad (6)$$
$$\approx \frac{T\left(x_i,t_j\right)+T\left(x_{i+1},t_j\right)}{2}\frac{x_{i+1}-x_i}{k_{eq}}$$

Case 2: When the entire cable segment is stationary, the strain and therefore the tension of the segment will not change, i.e.

$$\begin{aligned} &T(x_i,t_j) = T(x_i,t_{j-1})\ and\ T(x_{i+1},t_j) = T(x_{i+1},t_{j-1}). \\ &u(x_i,t_j) = u(x_i,t_{j-1})\ and\ u(x_{i+1},t_j) = u(x_{i+1},t_{j-1}). \end{aligned} \quad (7)$$

Case 3: A part of the cable segment is moving, while the rest of it is stationary. Assume that node *i* is moving, while node *i+1* is stationary. From (7), for the stationary section of the cable segment, $T(x,t_j) = T(x,t_{j-1})$ *and* $u(x,t_j) = u(x,t_{j-1})$. The displacement of the stationary section can be approximated by the displacement of the last moving point of the cable segment. Therefore, we can approximate that (6) holds true.

On moving one end of the cable initially only a part of the cable moves, and as the tension at the input end changes, motion gradually propagates across the cable. If the first *k* nodes are moving at some time instant t_p, we need to solve for the cable stretch and tension of the first *k* segments, solving *2k-1* equations simultaneously for tension of the first *k* nodes, and displacement of node *2* to node *k*. When the k^{th} cable segment satisfies eq. (5), motion propagates to the next node and node *k+1* becomes the last moving node.

C. Single Cable Simulation

Before simulating the closed loop system, simulations were carried out to characterize the tension transmission across a single cable. A desired motion profile is provided to the actuator end of the cable, and the tension at the two ends of the cable is calculated.

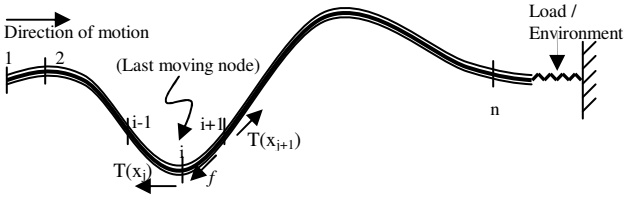

Fig 3: Discrete element model of a cable-passing through conduit

Simulation results are plotted in Fig. 4 for two cases: 1. Pretension is high such that the cable does not slack; 2. Pretension is low, such that the cable becomes slack during the motion. These simulation results are similar to the lumped mass model and experimental results performed Kaneko et al. [5, 6], which also justifies the assumption of negligible cable inertia.

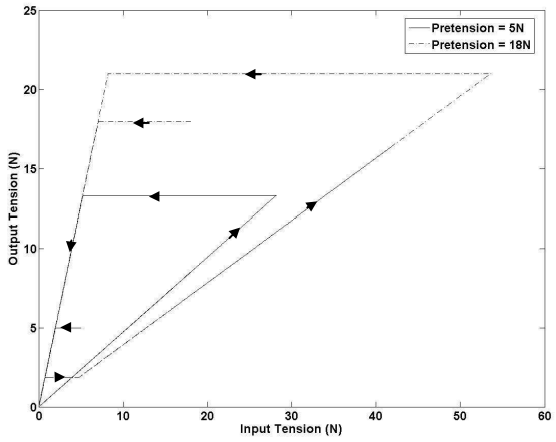

Fig 4: Tension transmission characteristics for two different pretension

It has been shown that due to tension losses across the cable, tension transmission may not be continuous across the cable. This leads to a period during which the movement of one end of the cable does not lead to the movement of the other end. The other end starts to move only when the tension change on the first end is significant enough to overcome friction. Thus it follows a backlash type of force transmission profile.

D. Closed loop cable-conduit Simulation

We extend the simulation of single cable to the case of closed loop system, assuming no slacking at the two pulleys. One end of each cable (cable *A* and cable *B* as shown in Fig 5) is fixed to the drive pulley while the other end is anchored to the follower pulley. Apart from the assumption of small cable motion, we can also assume that the nodes on one side of the pulley do not move to the other side. This assumption is reasonable since we always have some part of cable exposed without a conduit where no friction is acting, and therefore can be taken towards the compensation for the cable motion.

Similar to the case of single cable described above, the simulations are carried out with the constraints for torsional spring and no slacking at the pulleys,

$$\tau_o = -K_e\theta_o = (T_4 - T_2)R_o \tag{8}$$

$$x_3 - x_2 = 2R_o\theta_o \tag{9}$$

$$x_2 + x_3 = L \tag{10}$$

where τ_o is the torque being applied by the load motor, θ_o is its angular rotation, R_o is the radius of the pulley at the load motor, K_e is the simulated environment stiffness, L is the sum of two cable lengths (with pretension), $T_{1,2,3,4}$ denote the tension at the four ends of the cable, and $x_{1,2,3,4}$ denote the position of the corresponding ends.

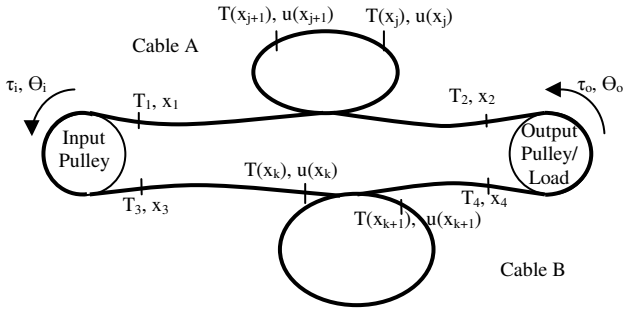

Fig 5: Model for the closed loop cable conduit system

The input motor is provided with a sinusoidal oscillatory motion profile. For each time step the motion of the input motor is calculated and based on that, we determine the '*last moving node'* on each side of the pulley, and the tension and displacements of all the nodes up to the last moving node. Consider the time period when one end cable *A* is moving, while the other end is stationary, i.e. there is some intermediate node on the cable *A* which is the last moving node. During this period, cable *A* will act as an independent cable, the motion of which will not affect the motion of cable B. Therefore during the time period when the last

moving nodes of the two cables do not coincide, there is no interaction between the two cables and the motion of the two cables can be solved independently. Once the last moving nodes of the two segments coincide, the entire system follows a collective motion. Based on the above analysis, the motion of the system can be divided in two categories, both sides of cable taut, or either side of cable slack. When one side of the cable goes slack the other side still moves as an independent cable.

E. Simulation Results Analysis

Apart from the backlash profile in motion and torque transmission, several other atypical phenomena are observed. Fig. 6 shows the variation in the tension at the two ends of the cable for both cables, input (load) torque vs output (drive) torque profile, and input vs output angular rotation. For the ease of understanding, various time instances in the motion and the sequence of motion propagation have been marked in Fig. 6, which are described as follows:

1. Drive motor starts to rotate counterclockwise such that cable *A* is getting stretched, while cable *B* is released.
2. Motion has propagated across cable *B* and it starts to move load pulley. Motion has only been propagated in cable *A* till some intermediate point, and a part of cable A is still stationary.
3. Motion has propagated to the end of cable *A*, and both cables start to move.
4. Cable *B* goes slack.
5. Input motor reverses its direction of motion, while cable *B* still remains slack, load pulley is not moving.
6. Cable *B* starts to move after getting taut again, and it moves the load pulley. Motion has only propagated in cable *A* till some intermediate point. Similar to stage 2.
7. Both cables start to move, but in direction opposite to that of stage 3.
8. Cable *A* goes slack.
9. Cable *A* remains slack, input motor changes direction of motion, similar to stage 5, but slack cable and direction of motion has been changed.
10. Cable *A* starts to move after becoming taut, and starts moving the load pulley. Similar to stage 6.
11. Both cables start to move again.

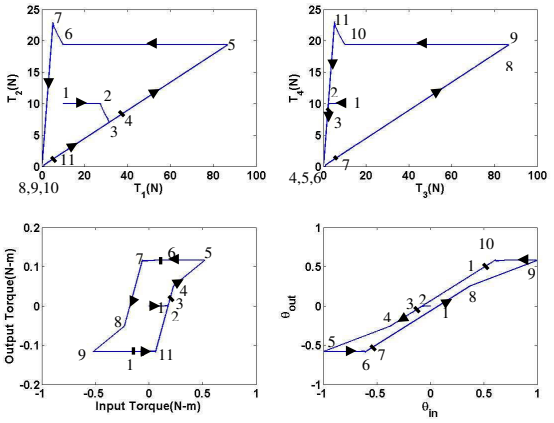

Fig 6: *Transmission profile* with various time instances

After stage 11, next stage coincides with stage 3, and stages 3-11 keep on repeating thereafter. Based on these stages the motion can be divided into following phases:

I. **Output pulley not moving** (Time interval between stages 1-2, 5-6, 9-10) – Motion has not propagated to the distal ends (i.e. the load pulley) in either of the cable. The load pulley remains stationary, and it translates to the backlash region in the transmission profile.

II. **One cable pulling another cable** (Intervals 2-3, 6-7, 10-11) – The tension variation at the two ends of the cable are opposite to each other, i.e. when tension at one end of the cable is increasing (or decreasing), but on the other end it is decreasing (increasing). This translates to the small slope in the torque backlash profile, which has also been referred as soft spring [3]. The motion of the output pulley is influenced only by one cable, while the other cable remains inactive. In this phase one of the cables is not moving, but it is not slack, i.e. the pretension is high enough to avoid any slacking.

III. **Both cables moving** (Intervals 3-4, 7-8, 11-3) - Entire system is moving collectively. This translates to the directly proportional part of the transmission profile.

IV. **One cable goes slack while other cable keeps moving** (Intervals 4-5, 8-9) - Since the motion is governed by one motor, similar to phase II, the slope in the torque as well as theta profile reduces.

V. **Change of direction of motion of one cable, while other cable remains slack** (Intervals 5-6, 9-10) - This can further be divided into two segments, 1. when the direction has not propagated to the distal end in the moving cable (the flat part) and 2. when one of the cables is moving while the other is not moving. While segment 1 is always present, segment 2 only appears in the case of *extremely* low pretensions.

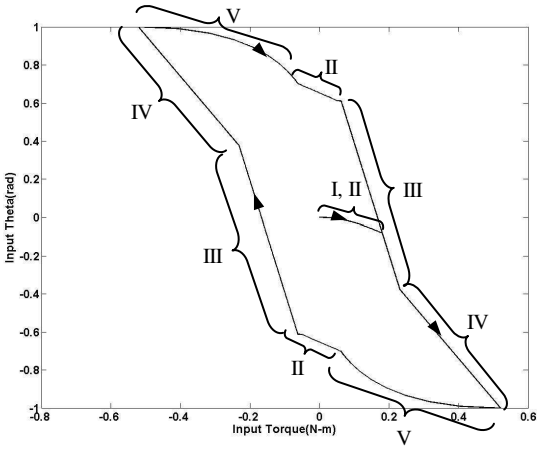

Fig 7: Input torque versus input theta with various phases

From these plots, it is evident that friction not only causes a backlash type of tension transmission profile, but also results in other phenomenon, such as changes in the slope of the transmission, introduction of small slopes in the torque transmission (intervals 6-7, 1-11), as well as opposite tension

variations at two ends of the cable. Apart form the transmission profile, all these phases are most predominantly visible in the plot of input torque versus input theta (Fig 7). This also provides evidence that if the state of the system friction is know, the motion of the load pulley and cables can be predicted based on the motion of the drive pulley.

IV. Experimental Results

To validate our simulation, experiments were performed using the setup described in Section II. The actuation cables were *0.52 mm* diameter, uncoated stainless steel *7x19* wire rope approximately *1.6 m* in length and wrapped around *12 mm* diameter motor pulleys. The stainless steel conduits were *1.2 m* in length, made from *0.49 mm* diameter wire wrapped into a close packed spring with an inner diameter of *1.29 mm*. The two motors were controlled using the dSpace control board. For this study, the pretension in the cables and shape of the conduit could was varied and controlled. Pulley angles were measured with a resolution of *0.72 deg*. Pulley torque was measured with an accuracy of *0.1 mN-m* over a range of *100 mN-m*, while the combined cable tension measured by the load cell had an accuracy of *0.1 N* over a range of *45 N*.

To correlate the experimental results with the simulation, several system properties were experimentally estimated. In particular, stiffness of the cable and conduits were measured to be *15.43 kN/m* and *137.76 kN/m*, respectively. Using (3), equivalent cable stiffness was calculated to be *13.88 kN/m*. Force relaxation or the creep of the cable was measured to be approximately *1.5 %*, with a time constant of approximately *30 sec* and therefore deemed negligible for these initial experiments. The friction coefficient between the cable and the conduit was measure to be *0.147*. Motor parameters including torque constant, motor inertia, coulomb friction and viscous damping were also estimated from experiments.

Fig.8 shows the experimental and simulation results for a pretension $T_0 = 7\ N$, and a half loop in the conduit. The trends are quite similar in the experimental and simulation results. The simulation results estimate experimental values with accuracy of *5-10 %*. The next sections show how the simulation and experimental results compared as the cable pretension and conduit path were varied.

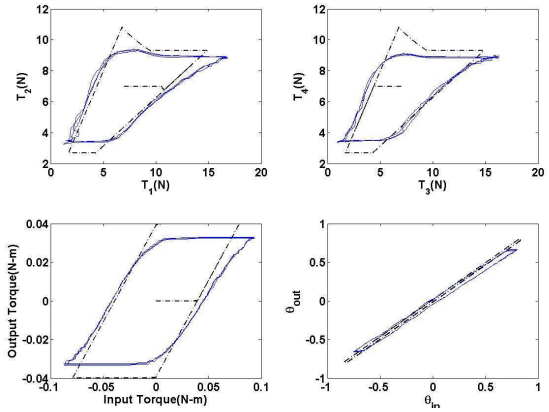

(a) Tension variation at the two ends of cable A and cable B, input torque vs output torque and input angular rotation vs output angular roation

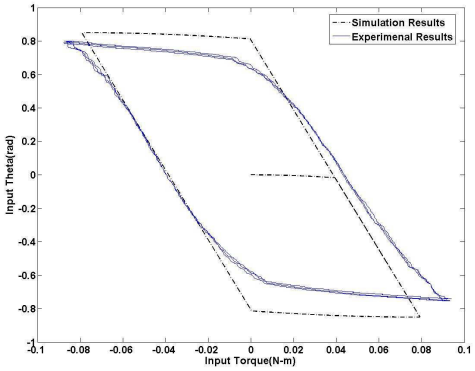

(b) Input torque versus input theta

Fig 8: Experimental and simulation results for T_0=*7 N*

A. *Variation of Number of Loops*

Friction is exponentially correlated to the curvature of conduit. For clarity in this experiment, the shape of the conduit was changed by adding additional '*loops*' or *360 deg* of bend. For introducing loops, entire length of the conduits was used such that the radius of curvature remained constant throughout the conduit. Increasing the number of loops should result in higher friction and hence, larger backlash width and lower load transmissions. Larger friction also leads to longer time periods when one of the cables is slack while the other cable is moving (fourth phase). The slope during this region also changes with the number of loops. The experimental results in Fig. 9 show similar trends with a good match in magnitudes of the motor torque.

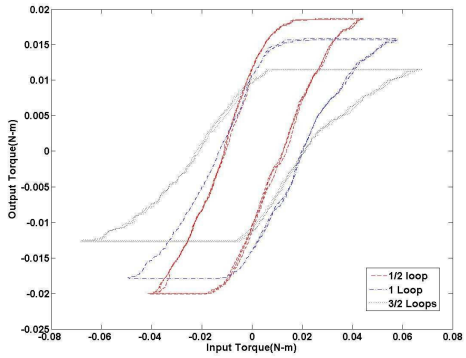

(a) Experimental results for different number of loops in conduit

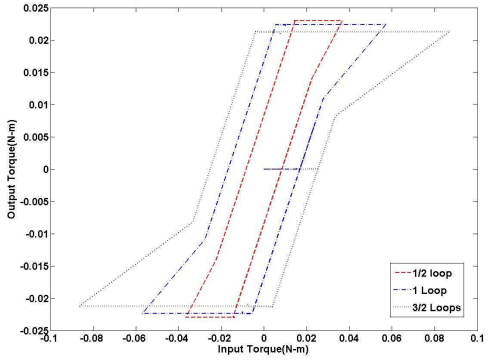

(b) Simulation results for corresponding number of loops

Fig 9: Variation in torque transmission with number of loops

B. *Variation of Pretension*

Since the tension loss is directly related to pretension (2), increasing the pretension increases the backlash. For a large pretension of *7 N*, cables do not slack, and therefore fourth phase is not present. For a pretension of *3.5 N,* fourth phase is present, when one cable goes slack while the other is still moving. This is also visible for *0.7 N* pretension, but in this case an additional trend is present showing the second segment of fifth phase, when one cable remains slack while the other cable is still moving. Fig 10 shows that the experimental and simulation results have similar trends with a close match in magnitudes of the torque profile.

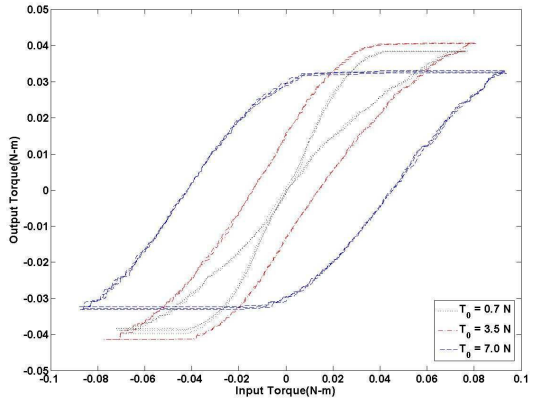

(a) Experimental results for different cable pretension

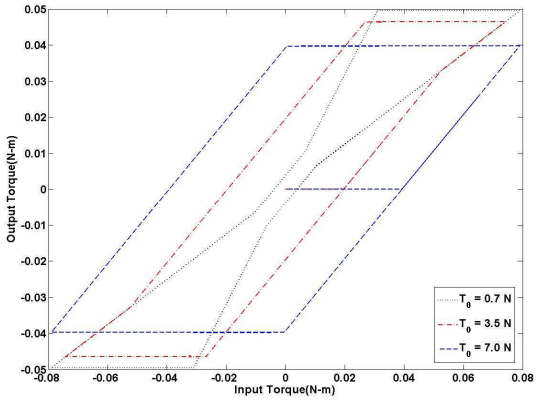

(b) Simulation results for corresponding variation in pretension

Fig 10: Variation in torque transmission with pretension in the cables

C. *Variation of Loop Radius*

According to eq. (5), tension variation across the cable is related to $\Delta x / R \doteq \Delta\theta$, therefore for a constant angle of curvature $\Delta\theta$, the simulation model predicts that there is no effect on system behavior based on the radius of a loop. To verify this, experiments were carried out for three different loop radii of *4.57 cm*, *6.35 cm*, *7.62 cm* while keeping the curvature angle same. Corresponding torque profiles are shown in Fig. 11. From the plots it can be inferred that the variation with the loop radius is negligible as estimated by the model.

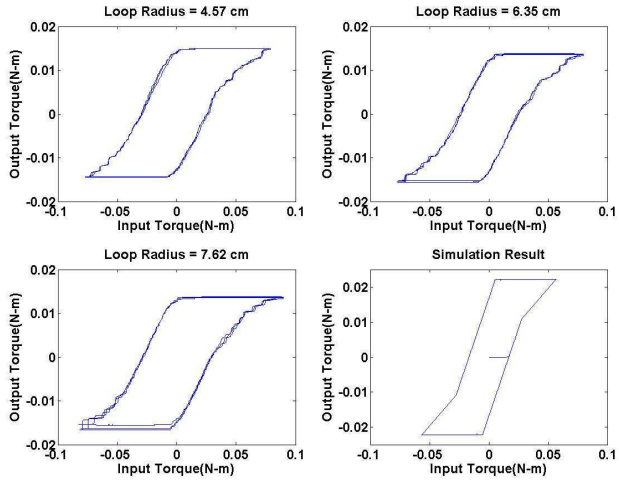

Fig 11: Variation in torque transmission with loop radius and corresponding simulation result

V. CONCLUSION

Overall, the simulations were successful in predicting the trends of the transmission characteristics in the experimental setup and closely approximating the resulting changes in forces and motion. A portion of the errors in the estimation can be attributed to inaccuracies in calculating the friction coefficient between the cable and the conduit and variations in the stiffness of the cable and the conduit. The model also neglects the effect of force relaxation, friction effects at the two pulleys, as well as placement of the loop along the conduit. Though loop placement will not affect the capstan effect, it will change the cable elongation, and will therefore change the overall profile. Though care was taken, kinks were inadvertently introduced in the cables, which also deteriorate the system performance.

REFERENCES

[1] G.S. Guthart and J.K. Salisbury, "*The Intuitive telesurgery system: Overview and applications*," in Proc. *IEEE Int. Conf. Robotics and Automation (ICRA2000)*, San Francisco, CA, April 2000, pp. 618-621.

[2] R.J. Fanzino, "*The Laprotek surgical system and the next generation of robotics*," *Surgical Clinics of North America*. Volume 83(6), pp. 1317-20, Dec 2003.

[3] Kaneko, M., W. Paetsch and H. Tolle, "*Input-dependent stability of joint torque control of tendon-driven robot hands*," *IEEE Trans. Industrial Electronics*, Vol. 39, Issue 2. pp. 96 – 104, April 1992.

[4] W.T. Townsend and J.K. Jr. Salisbury, "*The effect of coulomb friction and stiction on force control*," in *Proc. IEEE Int. Conf. on Robotics and Automation*, vol.4, pp 883-889, Mar 1987.

[5] Kaneko, M., M. Wada, H. Maekawa and K. Tanie, " *A new consideration on tendon tension control system of robot hands*," in *Proc. 1991 IEEE Int. Conf. on Robotics and Automation*, Sacramento, 1991, vol.2, pp 1028 – 1033.

[6] Kaneko, M., T. Yamashita and K. Tanie, "*Basic considerations on xtransmission characteristics for tendon drive robots*," *Int. Conf. on Advanced Robotics,* 1991, vol. 1, pp. 827 – 832 [*5th Annu. Conf. Robots in Unstructured Environments*, 1991]

[7] Palli G. and Melchiorri C., "*Model and control of tendon-sheath Transmission Systems*," in *Proc. IEEE Int. Conf. on Robotics and Automation, 2006.*

[8] Palli G. and Melchiorri C., "*Optimal Control of Tendon-Sheath Transmission Systems*," IFAC symposium of Robot Control, 2006